One or more of the F

LASER SATELLITE-TRACKING SYSTEM

Progress Report No. 2
Contract NSR 09-015-039

For the Period 1 February 1968 to 1 July 1968

August 1968

Prepared for
National Aeronautics and Space Administration
Washington, D.C.

Smithsonian Institution
Astrophysical Observatory
Cambridge, Massachusetts 02138

LASER SATELLITE-TRACKING SYSTEM

Progress Report No. 2
Contract NSR 09-015-039

For the Period 1 February 1968 to 1 July 1968

August 1968

Prepared for

National Aeronautics and Space Administration
Washington, D.C.

Smithsonian Institution
Astrophysical Observatory
Cambridge, Massachusetts 02138

808-49

TABLE OF CONTENTS

LASER SATELLITE-TRACKING SYSTEM

Contract NSR 09-015-039

INTRODUCTION

During the second report period (1 February 1968 to 1 July 1968) of contract NSR 09-015-039 awarded to the Smithsonian Astrophysical Observatory (SAO) for the purpose of developing a laser satellite-tracking system, additional progress has been made in research and experimentation with a prototype laser system.

Range measurements on laser satellites, demonstrating that the system performed as expected, were made shortly after the laser transmitter acceptance tests were completed. In addition, tests to determine the combined performance characteristics of the system were initiated. Problems with the laser transmitter, however, have so far prevented the start of a routine night observing program and completion of the major portion of the evaluation program.

The following sections deal primarily with our work during the report period. Included also is a more complete description of the prototype laser hardware than that in Appendix A of Progress Report No. 1.

The report contains five parts. Pare I gives a detailed description of the major components of the ranging system. Part II discusses the evaluation tests run to date with the hardware. Part III deals with some of the problems encountered in the prototype hardware. Part IV discusses the ranging observations from the prototype unit to date. Part V states our plans for the next report period.

PART I. PHYSICAL AND OPERATIONAL DESCRIPTION OF THE PROTOTYPE SYSTEM

The integration of the prototype system is shown in outline in Figure 1. The discussions to follow elaborate upon the operation of the system (photographs of the system appear as Figures 5, 6, and 7).

A. The Static Pointing Pedestal

The static pointing pedestal (see Figure 2) is a rotatable mount for pointing two instrument packages, a photoreceiver and a laser transmitter, to an overall positional accuracy of better than ± 1/2 arcmin. It employs a T-type elevation-over-azimuth configuration and is operated manually.

The azimuth axle is a conical weldment (on which the azimuth-axle housing rotates) mounted rigidly on a sole plate that is in turn anchored into a concrete pier. It serves as a solid support for two large-diameter precision ball bearings spaced approximately 4 ft apart. A worm gear against which the azimuth worm drives the azimuth-axle housing is attached to the upper end of this shaft.

Since the axle does not rotate and runs nearly the entire length of the azimuth-axle housing, it makes a convenient passage for electrical power leads to the readout-device lights. The lower end of the azimuth axle supports the stator of a slip-ring assembly. The rotor of the slip-ring assembly is carried on a hollow steel shaft connected at its upper end to the azimuth-axle housing. Power leads to the indicator-light transformers run from the slip ring up through this shaft.

The azimuth-setting circle, which is adjustable for alignment with true North, is also mounted to the upper end of the azimuth axle. This calibrated glass torus remains stationary in a horizontal plane.

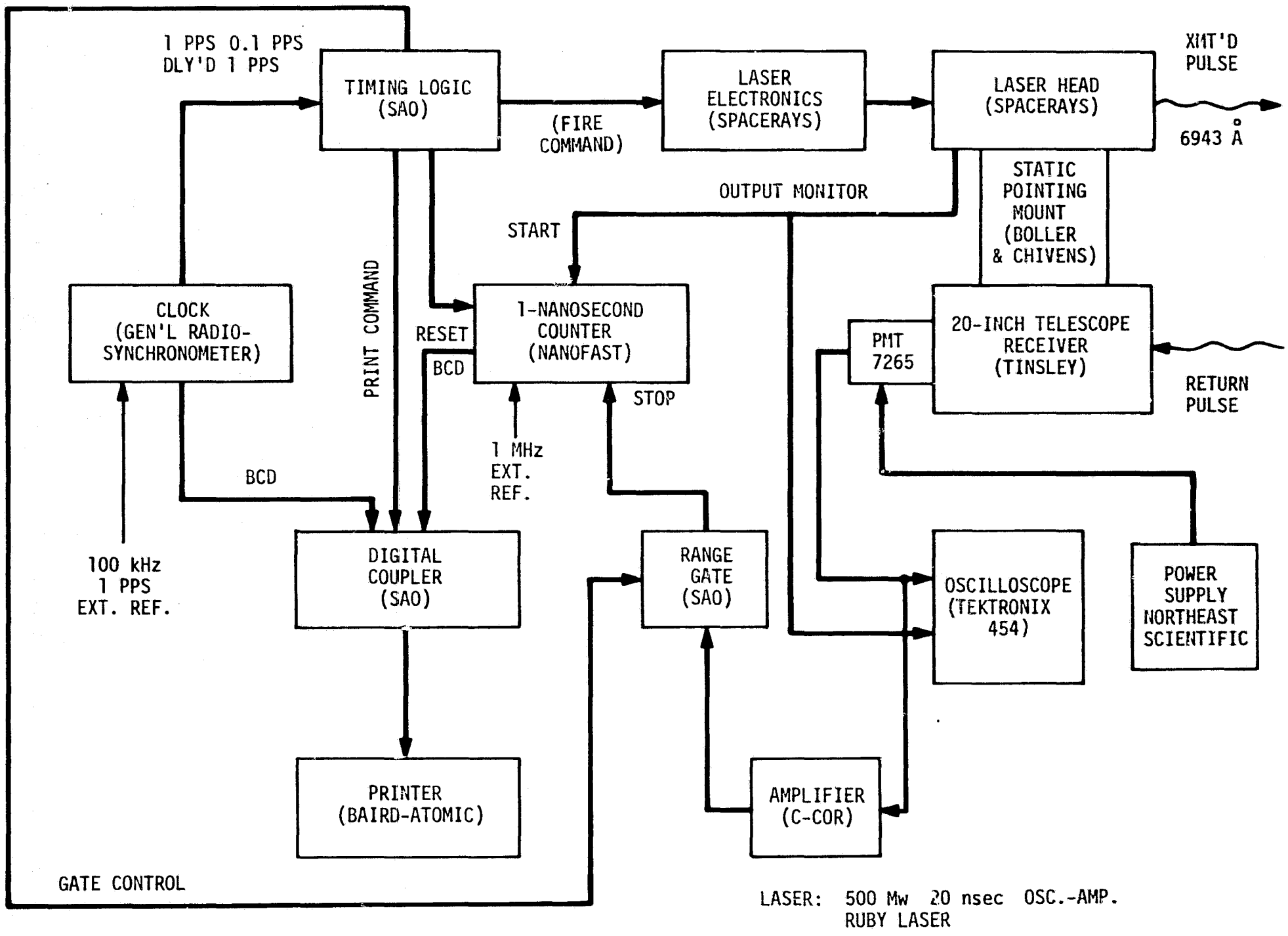

Figure 1. Prototype laser ranging system.

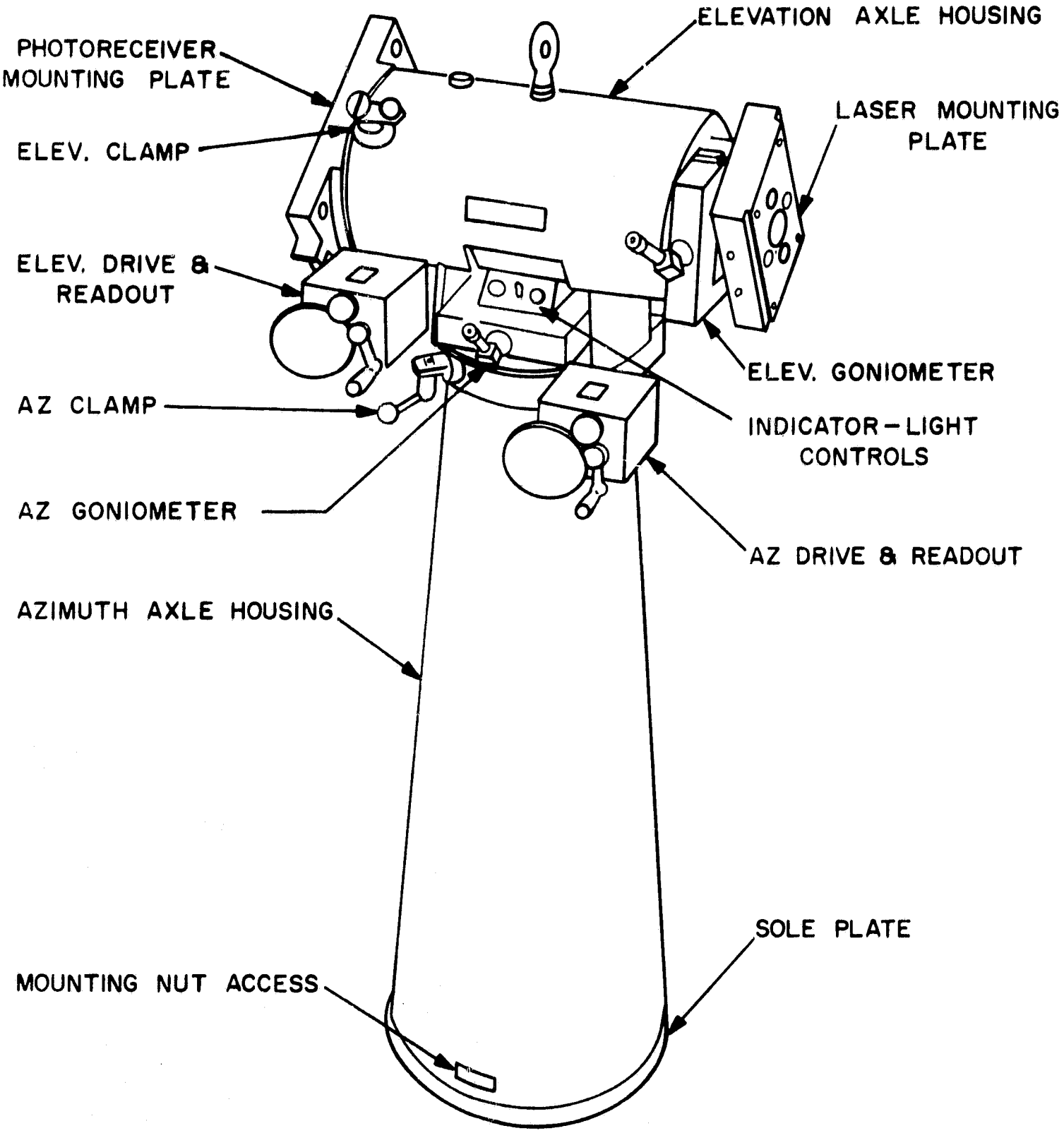

Figure 2. Laser static pointing pedestal.

A conical steel weldment supported by the precision bearings on the azimuth axle forms the azimuth-axle housing. It has unlimited rotation about the azimuth axle and forms the support for the elevation-axle housing and all instrumentation.

The azimuth-axle housing is driven by means of a worm drive assembly located at its top left side. The drive assembly contains a Veeder counter for coarse readout and a hand crank for power input. This unit can be modified to accommodate electric motor drive, if such were required in the future.

Three slots located around the bottom of the azimuth-axle housing provide access to the axle mounting nuts. Another access hole with cover plate provides access to the electrical connections to the slip-ring assembly.

A clamp prevents rotation of the azimuth-axle housing after the pedestal has been accurately positioned. It is located near the top of the housing convenient to the operator's left hand and is locked by turning the handle one-half turn clockwise.

The elevation-axle housing is a thick-walled steel cylinder bolted in a horizontal position to the flange on the upper end of the azimuth-axle housing. Two precision ball bearings, approximately one foot apart, support the elevation axle near either end. The supporting structure immediately beneath this cylinder forms a hollow area in which the switch, dimmer controls, transformers, and electrical junction points for the indicator lights are located. The goniometer (for fine readout of azimuth setting) is also located in this area.

A hand-driven worm drive assembly, similar to one previously mentioned, is located near the right end of the elevation-axle housing. The goniometer for fine readout of elevation setting is also mounted on this end of the housing.

A clamp similar to the one used for the azimuth axle also prevents rotation of the elevation axle. It is located near the top of the elevation-axle housing convenient to the operator's left hand and is also locked by turning the handle clockwise.

Supported on the bearings within its stationary housing, the elevation axle lies in a horizontal plane at the top of the pedestal. Made of steel, the major portion of the axle between the bearings is 6-1/2 inches in diameter and is reduced to 5-1/8 inches at both bearing shoulders. The center has been bored to a 1-1/2 inch diameter for convenient optical alignment.

As seen when facing the pedestal from the operator's position (see Figures 3), the left end of the elevation axle is flat to accommodate the photoreceiver mounting plate. This plate provides for a ± 2° elevation adjustment of the photoreceiver. By means of opposing adjustable screws, which between them accept a lug on the tube saddle, the position of the photoreceiver may be set with respect to the axle elevation. The worm gear for elevation drive is also on the left end of the axle within the housing.

The right end of the elevation axle is machined concave to accept a matching spherical convex portion of the laser mounting plate. This ball joint provides a ± 2° azimuth adjustment of the laser. The right end of the axle also carries the elevation-setting circle, which is adjustable for alignment with true horizontal.

B. The Laser Transmitter

The laser transmitter system provides a pulse rate of 1 per 30 sec. The transmitter package contains both an oscillator and an amplifier ruby-laser head, a Pockels-cell Q-switch, a Brewster stack polarizer, a rear reflector, optics for coupling the oscillator and amplifier rods, a set of beam-forming optics with facilities for boresighting, and an output monitor. All these units are mounted on an aluminum I beam (for arrangement of the components on the I beam see Figure 4). The ruby rods and flashlamps are water cooled and the cavities are purged with dry nitrogen during operation of the laser. The entire unit is protected by a dustproof cover (see Figures 5a and b).

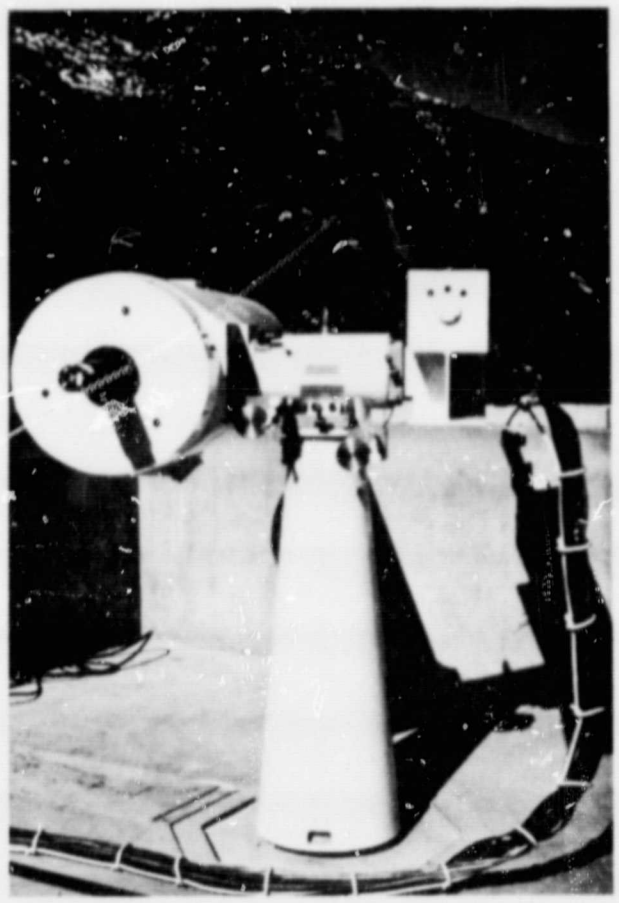

Figure 3a. The pedestal with the receiver (left side) and transmitter (right side) attached, Mt. Hopkins, Arizona.

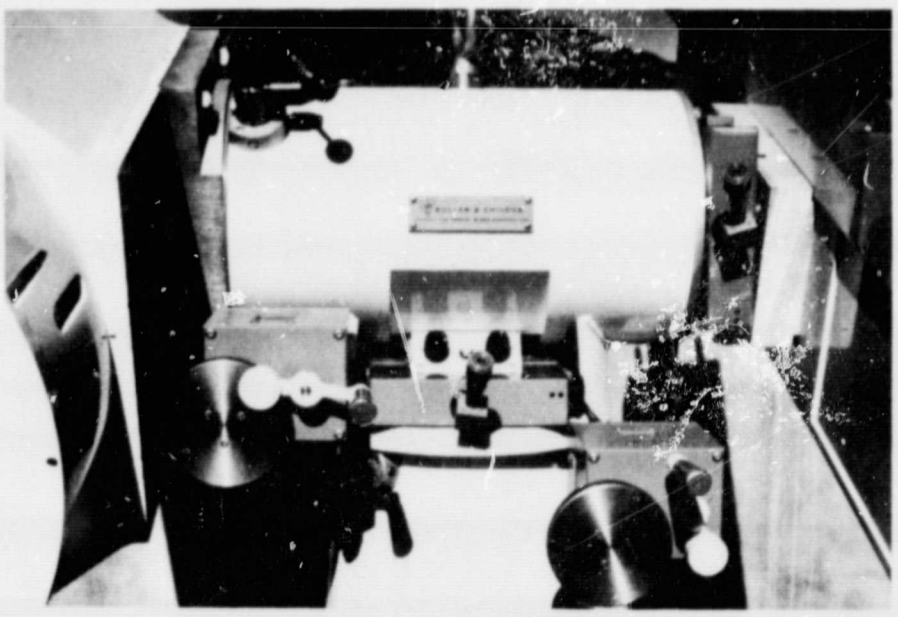

Figure 3b. Closeup of the pedestal control and readout area.

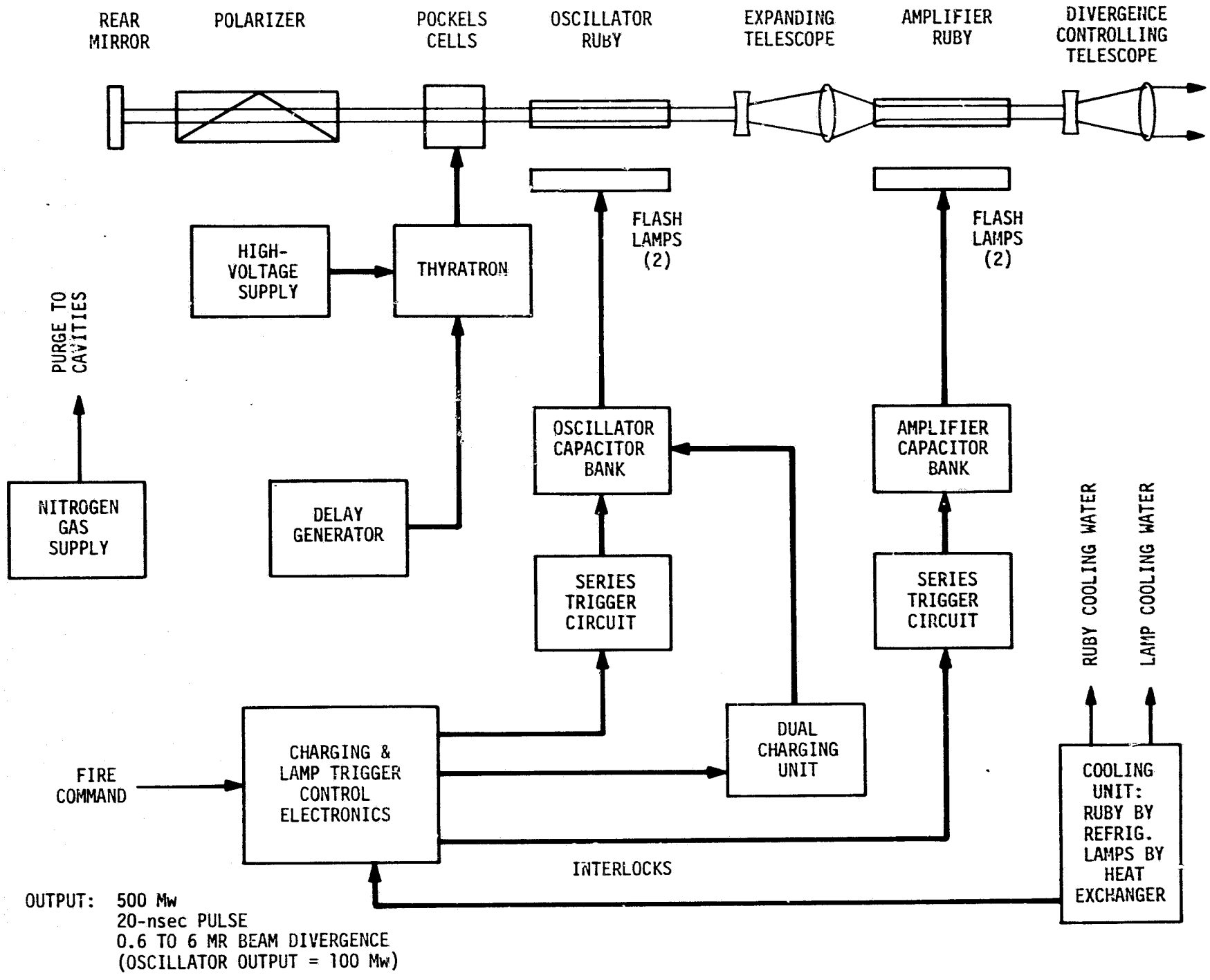

Figure 4. Laser transmitter.

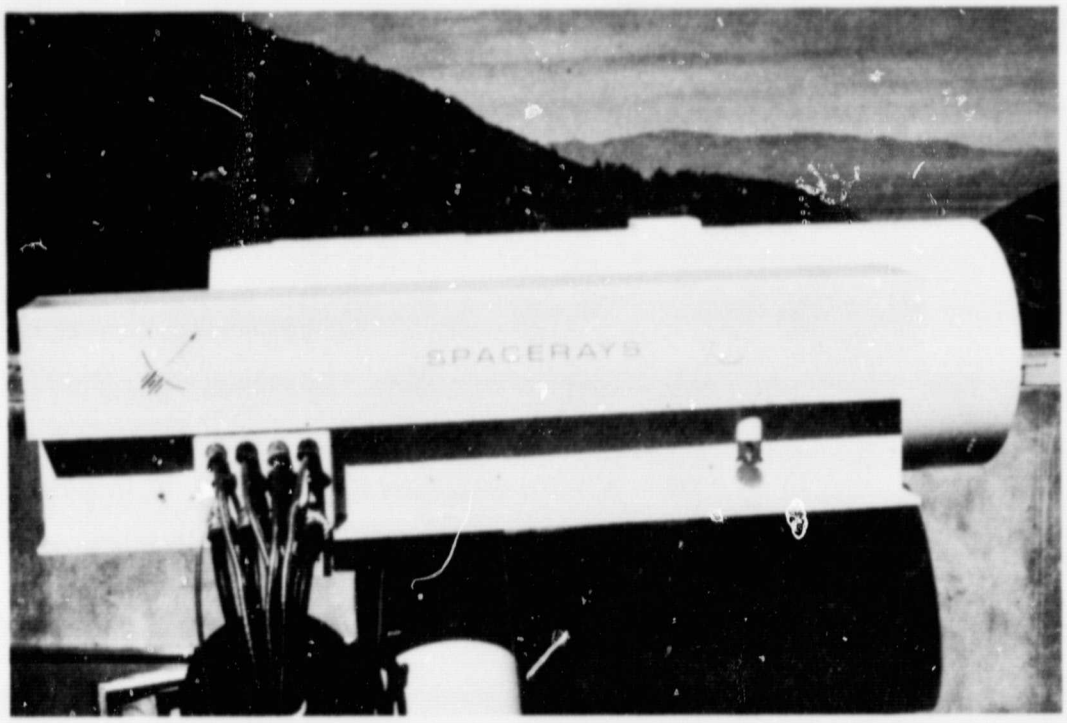

Figure 5a. Laser transmitter on the pedestal, showing cooling hoses and power and trigger cables.

Figure 5b. The laser transmitter with the dust cover removed.

The oscillator head contains two 6.5-inch xenon flashlamps and a ruby 3/8 inch in diameter and 6-5/8 inches long. The lamps are located at the focal points of an intersecting elliptical cross-section silver-coated cavity; the rod is located at the common focal point. Both flashlamps and the ruby rod are contained within individual quartz water jackets sealed with "O" rings. The amplifier cavity is arranged the same as the oscillator cavity, but utilizes a 5/8-inch-diameter, 7-inch-long ruby rod.

A Pockels cell containing a potassium deuterium phosphate crystal is used as the Q-switch. The Pockels cell is held at high potential to prevent firing of the laser until the proper time, then the potential is dropped to 0 volts in about 30 nsec. A giant pulse is formed up to 200 nsec later.

The beam-forming telescope consists of a Galilean lens and a 6-inch-diameter double convex lens. Both lenses are coated for maximum transmission at 6943 Å. The Galilean lens is fastened to a movable platform and can be moved by a micrometer attached to a flexible cable to vary output-beam divergence from 2 arcmin to 20 arcmin. An eyepiece unit, which can be inserted through the transmitter package cover into the beam-forming optics in front of the Galilean lens, is used with a fixture attached in front of the 6-inch lens, for boresighting the laser. The transmitter is fired and burns a hole in a target held in the boresighting fixture. Next, the eyepiece is inserted into the system, and the cross hair in the eyepiece is set onto the hole in the target, thus defining the center of the output beam. The boresighting fixture is then removed, and the laser can be brought into alignment with other components of the ranging system by sighting onto a convenient distant light source. The eyepiece is removed before the laser is again fired.

Alignment of the active and passive optical components is accomplished with a collimator. The collimator is fastened to the rear end of the I beam to align the oscillator rod, the Pockels cell, the Brewster stack, and the rear mirror. It is then moved to the front end of the I beam to align the coupling lens, the amplifier rod, and the beam-forming telescope to the oscillator section of the system. This system works well, permitting quick and accurate alignment of the components.

The output pulse monitor is an ITT diplanar photodiode with an S-20 cathode driven at -1000 v DC. The monitor is arranged to look at laser light reflected from the rear surface of the 6-inch lens of the beam-forming telescope. The pulse from this monitor starts the time-interval counter.

The transmitter assembly operates at 1 pulse per 30 sec. An input to the oscillator cavity of 6000 joules maximum and to the amplifier cavity of 9000 joules maximum can produce an output in excess of 500 Mw in a 20-nsec pulse, although the transmitter is not typically operated above the 500-Mw level.

C. The Telescope Photoreceiver

The telescope photoreceiver, designed primarily to be used with a photomultiplier tube (PMT), detects returning laser pulses. Equipped with an eyepiece, it permits visual checking of satellite positions, collimation of the receiver with the transmitter, and alignment of the readout devices on the pedestal with the receiver optical axis.

The receiver employs a coaxially folded, prime-focus optical system, and has separate optical subsystems for the eyepiece and the PMT. The primary subsystem is 20.5-inch parabolic mirror with a 6-inch hole in the center. The other is a 5-inch optical flat supported through a cored hole in the center of the mirror.

The eyepiece optical system (Figure 6a) operates, in essence, as any standard viewing telescope, with the eyepiece focused on the prime-focus plane. The only departure from a conventional system is the addition of a pair of relay lenses that transfer the image from the prime-focus plane to the side of the telescope tube and the eyepiece. A flip mirror deflects the light through the relay lenses to the eyepiece.

The optical system for the PMT, together with RCA 7265 tube (Figure 6b), gives an image of the primary mirror at the PMT face. Thus, instead of the PMT seeing at a point image of the turning laser light, the detection of which

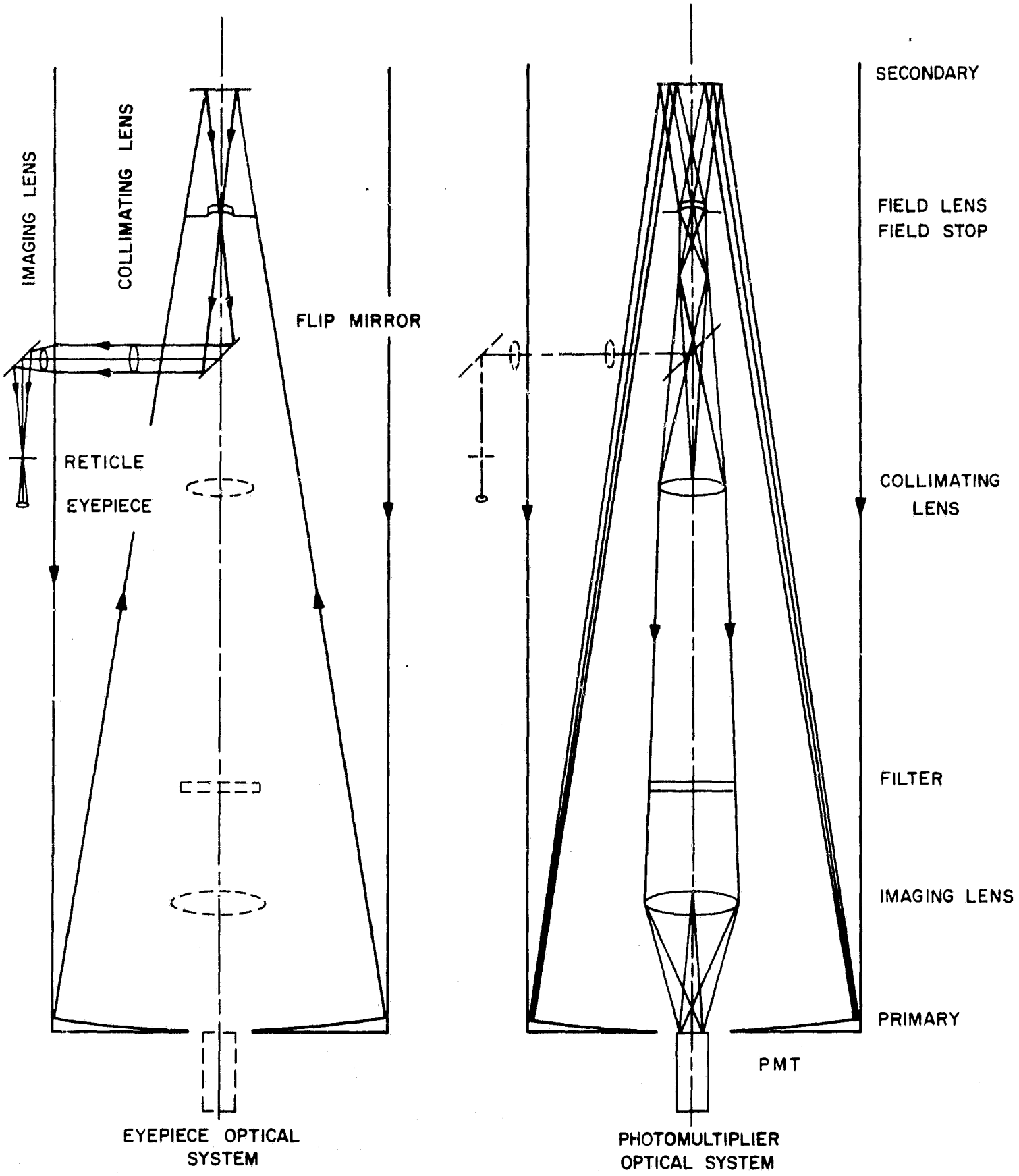

Figure 6. Optical system and ray pattern for the telescope photoreceiver.

might depend on where the image fell on the varying sensitivity of the photocathode, the PMT looks at a donut-shaped image of the uniformly illuminated primary mirror. In this way, the laser return is evenly distributed across the PMT cathode.

In order to provide the image of the primary mirror at the PMT face, a positive meniscus field lens with a 2-inch focal length is placed in the primary focal plane. The field lens forms an image of the primary mirror at a point slightly more than 2 inches behind the field lens. This image is then transferred through the hole in the primary mirror to the PMT face by a pair of relay lenses, a collimating lens, and an imaging lens. The collimating lens also collimates the light bundle so that the angle of incidence of the rays passing through the interference filter, set just in front of the imaging lens, does not exceed $\pm 1°$.

The field stops are located at the field lens position. The stops are holed disks that permit a field range from 2 arcmin to 20 arcmin in 2-arcmin increments. As the various stops are introduced into the optical system, a graduated reticle in the eyepiece checks changes in the field size. The field stops do not affect the diameter of the image of the primary mirror on the PMT face. In the latter case, only the intensity of the image is affected by the field stop changes.

A 6-Å passband interference filter is mounted into a tiltable holder inside the tube between the collimating lens and the focusing lens of the second set of relay lenses. The filter can be tuned by a micrometer (located at the back of the telescope), which adjusts the position of the tiltable holder.

The optical components in the system are coated to provide optimum performance in the spectral region in which they are used. The lenses in the eyepiece optical system are standard AR coated to provide good response in the visual regions. The lenses in the PMT optical system have a dielectric "V" coating to allow less than 0.3% reflectance at each air-to-glass surface at 6943 Å, the ruby-laser wavelength. The primary, secondary, flip, and

diagonal mirrors are surfaced with aluminum, overcoated with silicon monoxide. The efficiency of the PMT optical system including the primary and secondary mirrors is about 43%.

A closed tube, with two internal spider support systems, houses the entire optical system. The flip mirror for the eyepiece relay system and the field-stop selector are located inside the tube. A trap door in the side of the tube has been provided to operate the flip mirror and change field stops. The PMT assembly is fastened at the rear of the telescope on the primary mirror cell housing.

D. Ranging and Data Recording Electronics

The fundamental accuracy of both the epoch of the laser ranging pulse and its time-of-flight is derived from the standard station clock. This clock is a VLF-steered crystal oscillator system (EECo Model ZA 34685), which produces a variety of precision pulse rates, with digital accumulation and display. The accuracy of the station clock is maintained by means of the SAO master clock to within ±100 microsec of the UTC (USNO) time base. Short-term frequency stability is within 2 parts in 10^{10}.

For purposes of laser fire control and firing epoch recording, the 100-KHz output of the station clock is accumulated for time presentation by a timing synchronometer (General Radio Model 1121A). Station time is read in BCD format from the unit upon command. The synchronometer also produces timing pulses at rates of 1 and 0.1 pulse per second. These pulses are used in the SAO fire control unit in coincidence circuits that permit either (1) manual firing of the laser or (2) automatic firing of the laser at uniform, predetermined intervals. In general, the epoch of firing, for both modes, corresponds to precise 30-sec or 1-min markers of station time.

The fire-control unit produces a firing pulse to the laser power supply, which fires the laser. In addition, it provides appropriate pulses to reset the range counter and its associated range gate and to command the digital data printer. Figure 7 shows the fire-control circuitry and other components of the system.

Figure 7. From left to right: the EECo timing system, the ranging electronics (including the time-interval counter, oscilloscope, fire control circuitry and printer) and two cabinets housing the laser capacitor bank, the Q-switch driver, and pulse-forming networks. The laser cooling cabinet is not shown.

The range counter (Eldorado Model 783G or Nanofast Model 536) measures with high resolution (10 or 1 nsec depending on the counter) the time interval between the emission of the laser pulse and the detection of a return signal. The start pulse, corresponding to the laser pulse emission, is produced by a photodiode monitor located near the laser optics; the stop pulse is the photoreceiver signal after amplification in a fast-rise, low-time-delay amplifier (C-COR Model 1375T). The range counter derives its counting accuracy and resolution from a 1-MHz frequency reference supplied by the station clock.

To eliminate backscatter and other noise problems, the receipt of the stop pulse by the range counter is controlled by a range gate. The range gate remains closed until it receives a timing pulse, which is delayed an adjustable predetermined amount from the start signal. This delay may be

derived either from the synchronometer or from the internal counting logic of the range counter. Receipt of the signal opens the gate, permitting registration by the stop signal.

The epoch and range/time interval data are registered and stored in a BCD data format by the synchronometer and counter, respectively. After a suitable delay from the time of firing, the fire-control unit commands both to be printed on a 2-channel digital printer (Baird-Atomic Model QF-8).

The photoreceiver electronics consist of a selected photomultiplier of high quantum efficiency (RCA type 7265) in a shielded, low-noise enclosure (Nanoseconds Systems Model 57265). Anode voltage between 2200 and 2400 v is provided by a regulated supply (Northeast Scientific Model RE3002). Data recordings of the waveforms of the returned signals may be recorded with a high-speed oscilloscope/camera system (Tektronix 454A with C-40 camera). These photographs are useful for confirming returns and for diagnostic purposes.

The oscilloscope/camera unit is also used in conjunction with a fast-pulse detector (Spacerays FPD-125) to make power and energy measurements of the laser output.

PART II. PROTOTYPE-EVALUATION PROGRAM

Telescope receiver tests were made at Mt. Hopkins by measuring the voltage across a 570 K-ohm resistor in the output circuit of the photomultiplier as the stars Arcturus, Vega, and Altair drifted through the field of the telescope. The field aperture was 10 arcmin and the bandwidth was assumed to be 2 nm. The measured field values came out as follows:

Vega	7 arcmin
Altair	12 arcmin
Arcturus	10 arcmin.

The value of 12 arcmin is probably most nearly correct, because it was difficult to determine whether or not the star went through the center of the field with the flip mirror in the "up" position.

The sensitivity of the receiver was determined by computing V/ϕ from the measurements, where V is the output voltage of the photomultiplier in nv and ϕ is the light flux in photons m^{-2} sec^{-1} entering the receiver aperture. The quantity V/ϕ is proportional to the product of the effective area of the receiver and the gain of the photomultiplier tube. The results are compared below with other similar measurements made at SAO's other laser stations.

	V/ϕ		
	Vega	Altair	Arcturus
Mt. Hopkins	4	17	15
Organ Pass	40	54	31
Mt. Haleakala	2	--	7

The effective areas of the telescopes on Mt. Hopkins and on Mt. Haleakala can be estimated from the manufacturer's specifications. The effective area of the searchlight reflector at Organ Pass was determined by using the measured gain of the photomultiplier. The values are as follows:

	Effective area (m^2)
Mt. Hopkins	0.083
Organ Pass	0.060
Mt. Haleakala	0.052

When we compare these values with the values of V/ϕ, we see that the gain of the phototube used at Organ Pass may have been higher than either of the other two.

We now use the results described above to analyze two returns on which the signal strength was measured. These returns were reported as follows:

Return #4

Geos 2: Feb 23/68 03:39
Elevation 60°
Propagation time 9.13524 msec (R = 1.37 Mm)
Voltage 60 mv

Return #7

D1-D: Feb 23/68 04:10
Elevation 47°
Propagation time 10.19326 msec (R = 1.53 Mm)

The average value of V/ϕ from the measurements above is 12 nv photon^{-1} m^{-2} sec^{-1}. For a pulse duration of 15 nsec, a telescope aperture of 0.194 m^2, and a load resistor of 50 ohms (rather than the 570 K-ohms used for the star measurements), we obtain a calibration factor of 7.7 photons mv^{-1}.

For the present laser system, the range equations take the following form:

Geos 2: $\log S = 6.1 - 4 \log R$

D1-D: $\log S = 4.6 - 4 \log R$

For each return we compare the value of S determined from the measured voltage to the value calculated from the range equation. The measured values were lower than the calculated values by a factor that we call the excess signal loss. For the two returns the values of excess signal loss came out to be 29 dB for return #4 and 10 dB for return #7. The consistency with values obtained from the searchlight receiver at Organ Pass is interesting. It tends to confirm the fact that the excess signal loss is associated with the retroreflector rather than with the components of the laser system.

PART III. PROBLEM AREAS WITH THE PROTOTYPE LASER SYSTEM

During the evaluation program to date the following problems became evident:

1. Laser output instability, primarily because of high-frequency oscillation in flashlamp circuit and trapped air in ruby water jackets. A solution to this problem is being investigated.

2. Insufficient attenuation by laser range gate to prevent counter stoppages by backscatter or noise when high sensitivity is required. The gate was redesigned to provide greater rejection of large noise pulses.

3. Difficulty in aligning the laser and telescope for pointing direction. The problem is a result of non-color-corrected optics and mechanical design details, not the basic principles. Alternative means of aligning the laser to the telescope that do not depend on the optics are being investigated.

4. Transient problems (RFI) due to laser high-voltage trigger pulse. Solution was proper shielding and filtering.

5. Flip-mirror alignment in telescope is not positive and accurate. A hardware improvement is required.

6. Cable connections to mount are awkward and put considerable strain on connections. Better mounting brackets are required.

7. Maintenance procedures need to be simplified.

8. A spotting telescope with several degrees field of view mounted near the mount controls would eliminate considerable time in alignment. If equipped with an automatic shutter it could also be used for tracking unpredictable satellites such as Echo.

9. Mechanical mounting of laser component parts such as Pockels-cell resonance mirror, pile-of-plates polarizer, etc., must be improved so that alignment is not done with small coarse-thread machine screws.

10. Dust cover must be improved so as really to protect optical surfaces. Positive dry nitrogen pressure is probably required. Leak rate for such gas should be low enough to be economical in the use of tank nitrogen.

11. The Pockels cell should have a bigger chamber so as to provide a settling reservoir for particles produced by breakdown of liquid from light pulses and to provide for expansion due to temperature changes.

12. A special provision for bleeding air out of water system at some specially provided high point in the system should be supplied in the cooling water system.

13. Monitor of light pulses should not depend on condition of antireflection coating of front lens for calibration.

14. The following minor items are needed:

a. Suitable light shield around PMT in telescope.

b. Better communications system (loudspeaker in camera house).

c. Fixture to hold and illuminate predictions on mount.

d. Automatic control features to further guard against damage to laser, i.e., automatic adjusting lamp voltage limits; purge gas flow interlocks.

e. Light shield between laser and Baker-Nunn.

f. Fewer mechanical connections in laser lamp circuit (more soldered connections).

g. More indicator lights to indicate functions not ready for satellite ranging.

PART IV. OBSERVATIONS

The range observations obtained during February and June 1968 are tabulated in Table 1. The values for the month of June were obtained with the 1-GHz counter; its resolution is 15 cm. The other values were obtained with a 100-MHz counter (1.5-m resolution). The measurements were corrected for system delay but not for atmospheric delay or for the displacement between the laser system and the Baker-Nunn camera. Values of the temperature and pressure were recorded for each observation so that the atmospheric correction can be made eventually with a maximum error of only 5 cm. This correction is not needed for the present purposes, however, because the range measurements are being used with field-reduced, rather than precisely reduced, camera observations.

The predictions were made with the new AIMLASER program. The prediction errors were computed by rerunning AIMLASER after the measurement was obtained, to obtain a posterior prediction. The prediction error is the prior prediction minus the posterior prediction.

Only 30% of the errors were greater than 3 arcmin; consequently, the beamwidth of the laser could have been reduced from 10 arcmin to 6 arcmin with a 70% probability of a successful return. Such a reduction in the beamwidth would have been equivalent to almost a 3-fold increase in laser power.

The range residuals were all less than 370 m. These values are representative of errors in the field-reduced Baker-Nunn observations. The laser observations are expected to be considerably more accurate. Notice that the prediction error for the range is only an order of magnitude greater than the residual. This fact has an interesting consequence. The range residuals can be determined accurately enough at the observing station to decide immediately whether the observation is a good one, or whether a noise pulse was received and whether the threshold setting should be increased for subsequent measurements.

Table 1. Range observations.

Satellite designation	Date and time (UT)	Predictions Az (°)	Predictions El (°)	Predictions R (km)	Measured range (km)	Residual range (km)	Prediction errors range (km)	Prediction errors angle (arcmin)	Counter resolution (m)	"Satellite is sunlit"
6406401	Jun 6 $10^h46^m00^s$	343.58	53.92	1272	1272.2180	+0.17	0	1	0.15	no
	10 48 00	216.53	81.68	1074	1074.0473	-0.04	0	2	0.15	no
6503201	Feb 23 11 07 00	115.07	41.12	1439	1439.9573	0.18	-1	2	1.5	no
	12 56 00	266.54	27.60	1846	1847.1880	-0.10	-1	1	1.5	no
	13 00 00	348.09	61.42	1203	1203.8453	-0.19	-1	2	1.5	no
	13 02 00	36.64	43.15	1493	1492.9202	-0.10	0	3	1.5	no
	Feb 24 12 21 00	42.57	47.77	1368	1368.8556	-0.20	-1	2	1.5	no
	Jun 9 5 31 00	156.97	50.90	1212	1212.3254	0.35	0	1	0.15	yes
	5 32 00	145.37	37.87	1442	1442.3324	0.37	0	1	0.15	yes
	5 34 00	136.35	20.04	2054	2055.2915	0.30	-1	1	0.15	yes
6508901	Jun 6 10 09 00	332.17	35.23	2308	2308.1336	-0.10	0	1	0.15	no
	10 11 00	338.39	54.28	1898	1898.2503	-0.05	1	1	0.15	no
	10 13 00	9.08	77.10	1712	1712.5757	0.04	0	1	0.15	no
	10 15 00	118.63	70.93	1815	1816.2296	0.12	-1	1	0.15	no
	10 17 00	134.33	51.17	2161	2161.7457	0.14	0	1	0.15	no
	10 21 00	141.04	25.67	3208	3208.5522	0.12	-1	1	0.15	no
6701101	Feb 24 11 51 00	354.95	56.41	1551	1552.2941	0.85	0	4	1.5	no
6701401	Feb 23 4 04 00	278.54	20.58	2060	2062.4045	-0.11	-2	5	1.5	no
	4 06 00	294.52	37.46	1559	1560.0962	-0.18	-1	6	1.5	no
	4 10 00	27.11	47.45	1531	1527.9210	-0.18	3	6	1.5	yes
	4 12 00	49.15	32.94	1998	1994.8223	-0.09	3	4	1.5	yes
	Feb 25 3 51 00	13.53	46.83	1432	1430.5079	-0.12	1	2	1.5	yes
	Feb 26 3 39 00	310.84	35.42	1505	1503.5538	-0.23	1	4	1.5	no
6800201	Feb 15 2 54 00	78.67	66.77	1368	1368.3628	0.02	0	1	1.5	no
	Feb 17 3 33 00	278.37	69.40	1334	1334.5488	0.01	-1	1	1.5	no
	Feb 23 3 35 00	172.55	44.83	1661	1661.0543	0.05	0	1	1.5	no
	3 39 00	315.83	59.58	1369	1369.3277	-0.00	-1	1	1.5	no
	Feb 24 3 56 00	228.03	55.47	1448	1447.5721	0.02	0	1	1.5	no
	3 57 00	260.56	57.27	1410	1410.2704	-0.03	0	1	1.5	no
	3 59 00	305.29	41.22	1666	1665.3039	-0.10	0	1	1.5	no
	Jun 7 5 56 00	138.46	28.93	2230	2229.2348	0.17	1	2	0.15	yes
	5 57 00	133.87	37.50	1951	1949.8249	0.18	1	2	0.15	yes
	5 58 00	126.03	47.72	1718	1717.5303	0.18	0	3	0.15	yes
	5 59 00	110.72	58.85	1554	1554.0371	0.16	0	4	0.15	yes
	6 01 00	37.04	65.04	1515	1515.3345	0.02	-1	3	0.15	no
	6 03 00	0.92	45.33	1853	1853.3567	-0.07	0	2	0.15	no
	Jun 9 6 36 00	178.51	47.45	1722	1719.9629	0.13	2	6	0.15	yes
	6 39 00	277.85	72.34	1454	1454.4457	-0.00	-1	5	0.15	no
	6 40 00	308.72	61.31	1568	1568.7930	-0.06	-1	7	0.15	no
	6 41 00	320.20	49.47	1764	1765.2809	-0.10	-2	6	0.15	no
	6 42 00	325.80	39.44	2017	2019.1431	-0.12	-3	4	0.15	

PART V. PLANS FOR EVALUATION PROGRAM COMPLETION

During the completion phase, as many range measurements as possible will be made. They will be attempted when the satellites are sunlit as well as when they are in the earth's shadow. Measurements will be made before sunset and after sunrise, gradually extending as far into full daylight as the system permits. The accuracy of the range measurements will be studied as a result of using a counter of 1-nsec resolution (equivalent to 15 cm range). The laser observations will also be used in computing predicted azimuth and elevation settings for new observations. The extent to which the predictions can be improved is an important factor in designing a laser system, because it determines the beamwidths of the transmitter and receiver.

In addition to satellite ranges, the intensities of the laser returns will be measured. The reflecting arrays on present satellites are made of hundreds of cube corners. These introduce a randomness into the returns and make a statistical study necessary if the overall performance of the system is to be understood. Returns from a given range seem to fit a geometric distribution, one in which the standard deviation is a large fraction of the mean, or, in other words, one in which the relative fluctuation is large even for strong signals. It is important to study these fluctuations because in some cases signals may be 30 dB lower than values obtained by using the intensity of the radar return equation.

The definitive determination of the accuracy of a laser system involves the use of a network of systems and the calculation of precise orbits. An estimate of the system's accuracy can be made, however, in another way. The laser is fired at a ground target located at a fixed position. The laser is fired many times and the range is measured with each firing. The values of range obtained in this way have a random variation; its standard variation will denote the accuracy of the system. If N measurements are averaged, the average should have $N^{-1/2}$ times the error of a single measurement.

This relation holds until the level of nonrandom (systematic) errors is reached. Tests will be performed to determine the magnitude of the error that remains after full use is made of statistical averaging.

Before the evaluation of the system is completed, a measurement of the overall performance of the laser and telescope should be made. The laser output can be evaluated by photographing its beam as reflected from a diffusely reflecting distant target. Two cameras will be used to allow the effect of interference of the coherent radiation to be estimated. The spot size on the target determines the laser's beamwidth; and a density measurement of the film, its energy distribution. The efficiency and beamwidth of the telescope can be evaluated by measuring the phototube current as bright stars are allowed to drift through the field of view.

A particularly interesting measurement would be the range to the satellite Echo 2. This satellite does not have the diffuse surface that is thought to produce the scintillation in the returns from the other satellites. A difficulty arises because the orbit of Echo 2 cannot be obtained as accurately as that of the other satellites; consequently, the predictions for the azimuth and elevation settings may not be good enough. But the experiment is worth trying, particularly if a recent time correction can be obtained from another observing station.